Structural and electronic properties of Ni_2MnGa

S. R. Barman,[1,*] S. Banik,[1] and Aparna Chakrabarti[2]
[1]*UGC-DAE Consortium for Scientific Research, University Campus, Khandwa Road, Indore, 452017, Madhya Pradesh, India*
[2]*Solid State Laser Division, Centre for Advanced Technology, Indore, 452013, Madhya Pradesh, India*
(Received 27 March 2005; published 8 November 2005)

The equilibrium structure and electronic properties of a ferromagnetic shape memory alloy Ni_2MnGa have been studied for both the martensitic and austenitic phases by the full potential linearized augmented plane wave method. We report the stable martensitic phase at $c/a=0.97$ and the lattice constants are in good agreement with the experimentally reported values. The Ni $3d$ e_g related minority-spin peak in the density of states (DOS) near the Fermi level (E_F) in the austenitic phase splits into Ni $3d_{z^2}$ and $3d_{x^2-y^2}$ states in the martensitic phase. The minority spin DOS at E_F varies with c/a, while the majority spin DOS at E_F remains almost unchanged.

DOI: 10.1103/PhysRevB.72.184410 PACS number(s): 75.50.Cc, 71.15.Nc, 71.20.Be

I. INTRODUCTION

Ni_2MnGa has generated tremendous interest in recent years because of its potential application as a magnetically driven shape memory alloy that is more efficient than temperature or stress driven shape memory devices. Ni_2MnGa is ferromagnetic at room temperature and martensitic transition in this compound was first reported by Webster *et al.*[1] Recently, the highest known magnetic field induced strain up to 9.5%, giant magnetocaloric effect and large negative magnetoresistance have been reported in this system.[2–5] The crystal structure of Ni_2MnGa influences both its magnetic and micromechanical properties. In particular, the lattice constants determine the magnetic-field induced strain.

For Ni_2MnGa, the martensitic start temperature (T_M) is reported to be around 210 K, while the Curie temperature (T_C) is around 370 K.[1] In the high temperature austenitic phase, the structure of Ni_2MnGa has been found to be cubic $L2_1$ with $a=5.825$ Å from x-ray and neutron diffraction studies.[1,6] The structure can be visualized as a bcc lattice with Ni atoms at the corner sites and Mn and Ga atoms alternately in the center of it. From neutron powder diffraction it has been reported that in the martensitic phase, Ni_2MnGa undergoes a tetragonal distortion with $a=5.92$ Å, $c=5.56$ Å and $c/a=0.936$ [Fig. 1(a)] in the *Fmmm* space group.[1,6] Using x-ray diffraction, Martynov *et al.*[7] reported the lattice parameters to be $a=b=5.9$ Å and $c=5.54$ Å ($c/a=0.94$) using the same space group. Extra weak peaks with intensity $<3\%$ of the main peaks have been assigned to an additional modulation in the structure with five or seven layer periodicity resulting from a periodic shuffle of the (110) planes along the $[1\bar{1}0]$ direction.[1,7] Recently, detailed analysis of high resolution neutron powder diffraction pattern[8] reveals that the martensitic phase has a 7-layered orthorhombic structure with *Pnnm* space group, the lattice constants being $a_{Pnnm}=4.21$ Å, $b_{Pnnm}=29.3$ Å, $c_{Pnnm}=5.55$ Å. These lattice constants are related to the *Fmmm* space group unit cell by $a_{Pnnm}=(1/\sqrt{2})a_{Fmmm}$, $b_{Pnnm}=(7/\sqrt{2})a_{Fmmm}$, and $c_{Pnnm}=a_{Fmmm}$ giving c_{Fmmm}/a_{Fmmm} or c/a to be 0.932. Thus, while the periodicity of the modulation might depend on sample composition and preparation history, it is fairly well established from above XRD and neutron diffraction studies that the *Fmmm* unit cell has c/a ratio of about 0.94.

While there is general agreement about the experimentally determined structure of Ni_2MnGa (especially the c/a ratio) in the martensitic phase,[1,6–8] the situation is not so clear from theory.[9–16] There is disparity between different theoretical studies about the lattice constants of the martensitic phase. Godlevsky and Rabe using local spin density pseudopotential calculations, obtained the total energy (E_{tot}) minimum at $c/a=1$, with other shallow local minima at 1.08 and 1.2.[9] On the other hand, Ayuela *et al.* optimized the lattice constants using full potential linearized augmented plane wave (FPLAPW) method and found $c/a=1.16$.[12] In a latter publication, Ayuela *et al.* performed more accurate FPLAPW calculations and found the E_{tot} minimum around $c/a=1.25$, and claimed existence of a local minimum around 0.94.[13] Recently, Zayak *et al.* using the pseudopotential method, have considered a model structure with fivefold modulation, and found minimum E_{tot} at $c/a=0.955$.[16] However, this is not the global minimum since the E_{tot} minimum for the nonmodulated structure at $c/a=1.25$ is reported by them to be four times more stable than the modulated structure.[16] Thus, till date no theoretical calculation has reported a global minimum in E_{tot} at $c/a<1$ for the martensitic phase. This is in gross disagreement with experiment, which reports $c/a=0.94$. Structures with $c/a>1$ are obtained only

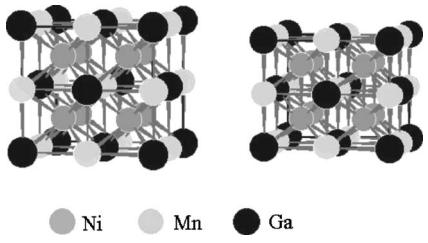

FIG. 1. The crystal structure of Ni_2MnGa in austenitic (left panel) and martensitic (right panel) phase. The tetragonal distortion in the martensitic phase is magnified to highlight the structural difference between the two phases. The modulation in the martensitic phase is not shown.

for nonstoichiometric and stressed samples.[1,6,7,17,18] This unsatisfactory situation has not been resolved until this date.

Heusler alloys are considered to be ideal local moment systems. In Mn based Heusler alloys (X_2MnY), the magnetic moment is mainly localized on Mn. The localized character of the magnetization results from the exclusion of minority-spin electrons from the Mn 3*d* states. The occupied *d* states of Mn are delocalized by their strong interaction with the *X*-atom *d* states.[19] Since, the Mn-Mn distance is $\geqslant 4$ Å, there is no significant direct interaction between the Mn atoms. RKKY type indirect exchange interaction gives rise to magnetism in this material. When the interaction is mediated by the *X* conduction electrons, the alloy is ferromagnetic and if it is mediated by the *Y* conduction electrons, it can have either sign, depending on the position of the Fermi level (E_F) in the Mn-Y *p-d* hybrid states. In Ni_2MnGa, which is ferromagnetic, the Mn-Mn interaction is mediated by the Ni conduction electrons.[19] Webster *et al.* reported the total magnetic moment of Ni_2MnGa to be $\approx 4.17\ \mu_B$ with $\approx 3.84\ \mu_B$ localized on Mn and $\approx 0.33\ \mu_B$ on Ni from magnetization and neutron diffraction studies. On the other hand, Brown *et al.*[20] reported 2.74 μ_B magnetic moment for Mn and 0.24 μ_B for Ni from polarized neutron measurements. Compton scattering supported by theoretical calculations using FPLAPW has been employed to study the magnetic moments in Heusler alloys like Co_2FeGa and Ni_2MnSn.[21] For Ni_2MnSn, the Mn moment was found to be 4.39 μ_B while the Ni moment was negligible.[21] For Cu_2MnAl, Compton scattering gave the Mn moment to be 3.25 μ_B,[22] which is in agreement with that reported by Deb *et al.*[21] X-ray magnetic circular dichroism (XMCD) in different Mn based and related Heusler alloys have been studied by different groups who found sizable orbital angular momentum component to the magnetic moment.[23]

In this paper, we report results of detailed FPLAPW calculations for Ni_2MnGa to obtain the equilibrium lattice constants corresponding to minimum E_{tot}. Until now in order to explain the absence of a global minimum at $c/a<1$, different theoretical studies have assigned the $c/a<1$ structure to be due to either nonstoichiometry, modulation, shuffle or distortion.[9,16] However, there are shape memory alloys which exhibit stable martensitic phase in the intrinsic structure, without consideration of the above effects. For example, NiTi and PdTi undergo martensitic transition from the B2 to B19′ and B19 structures, respectively, and FPLAPW calculations calculations clearly show that the martensitic phase is stable .[24] Hence, it is reasonable to expect that a tetragonal distortion to the $L2_1$ structure of Ni_2MnGa will be energetically stable and our work shows that this is indeed so with $c/a<1$. Using a rigorous approach with sufficient accuracy, we obtain the global E_{tot} minimum around $c/a=0.97$ with $a=11.11\pm0.03$ a.u. (5.88 Å) and $c=10.78\pm0.03$ a.u. (5.70 Å), which are in good agreement with the experimentally determined lattice constants. Moreover, the cubic and the tetragonal phases have similar volumes, as is expected for a shape memory alloy. The equilibrium martensitic phase is stable compared to the equilibrium austenitic phase by 3.6 meV/atom. We report the calculated magnetic moments for the equilibrium structures of both phases. Interesting changes in the density of states (DOS) are observed in the Ni 3*d* dominated DOS near E_F.

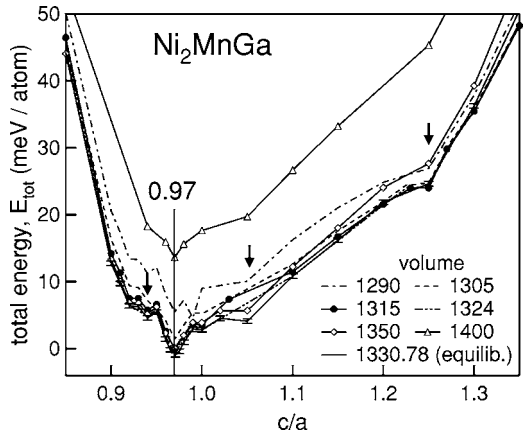

FIG. 2. The total energy (E_{tot}) of Ni_2MnGa in the martensitic phase as a function of c/a for different unit cell volumes. The accuracy of E_{tot} is shown as error bars on the equilibrium volume curve (solid line).

II. METHOD

The *ab initio*, relativistic, and spin-polarized FPLAPW calculations were performed with generalized gradient approximation[25] for the exchange correlation using the WIEN97 code.[26] Generalized gradient approximation (GGA) was used because it accounts for the density gradients which are neglected in the local density approximation. Moreover, it has been shown that for Heusler alloys GGA provides a better overall agreement with experiment compared to the local density approximation (LDA).[27,28] An energy cut-off for the plane wave expansion of 16 Ry is used ($R_{MT}K_{max}=9$). The maximum l (l_{max}) for the radial expansion is 10, and the maximum l for the nonspherical part ($l_{max,ns}$) is 6. The cut-off for charge density was $G_{max}=14$. The muffin tin radii were taken to be Ni 2.2488 a.u., Mn 2.3999 a.u., and Ga 2.2488 a.u. The number of k points for self-consistent field cycles is taken in 8000, which resulted in 641 k points in the irreducible part of the Brillouin zone. All the other parameters were kept at the default values generated by the WIEN97 code. The calculations were performed with the convergence criterion for E_{tot} to be 0.1 mRy, i.e., the accuracy of E_{tot} is ±0.025 mRy/atom (±0.34 meV/atom). This number is an order of magnitude smaller than the E_{tot} variation observed in Fig. 2; for example, the stabilization of the $c/a=0.97$ minimum is about 3.8 meV/atom w.r.t. $c/a=1$ for the equilibrium volume (Fig. 2). Moreover, some calculations were performed with even higher accuracy of 0.01 mRy. The change in E_{tot} between 0.1 and 0.01 mRy convergence criterion was 0.001 mRy/atom or 0.0136 meV/atom, which is not significant. So, all the calculations were done with 0.1 mRy convergence criterion. The E_{tot} value for each calculation is fully converged starting from initial crystalline charge density in each case. For the austenitic phase, the $Fm\bar{3}m$ space group is used with atomic positions 8*c* (Ni), 4*b* (Mn) and 4*a* (Ga).[1,6] For the martensitic phase, *Fmmm* space group is used with atomic positions: 8*f* (Ni), 4*b* (Mn), and 4*a* (Ga).[1,6] The calculations are done over a finer step (0.01) of c/a value between 0.9 and 1.0, where the E_{tot} minimum is expected.

III. RESULTS AND DISCUSSION

In order to obtain the lattice constants of the martensitic phase of Ni_2MnGa, E_{tot} is calculated as a function of c/a for different unit cell volumes including the experimentally reported[1] volume 1315 a.u. (Fig. 2). Considering different volumes around the experimental volume, we find the E_{tot} global minimum at $c/a=0.97$. It is interesting to note that all calculations for different volumes (1290 to 1400 a.u.) exhibit the 0.97 minimum. We also obtain a local minimum at $c/a=0.94$ (arrow in Fig. 2), although not for all constant volume curves. This local minimum is higher in energy than the 0.97 minimum by 5.5 meV/atom. Two other shallow local minima are obtained at $c/a=1.05$ and 1.25, but these are at higher energy with respect to the 0.97 minimum by about 5 and 23.8 meV/atom, respectively. Similar local minima at $c/a=1.08$ and 1.2,[9] and at 0.94 (Ref. 13) have been reported earlier. The overall shape of the E_{tot} curves in Fig. 2 are in agreement with Ref. 9, although they found the equilibrium value of c/a to be 1. A possible reason why Ref. 9 did not obtain the minimum at $c/a<1$ could be related to the use of LDA by the authors. We have used GGA because it has been shown that GGA gives better overall agreement with experimental data for Heusler alloys compared to LDA.[13,27,28] For Co_2MnX (X=Si,Ge,Sn), Picozzi *et al.* find that GGA is essential for an accurate description of the equilibrium volumes and of the electronic and magnetic properties of these systems.[27] Moreover, Ayuela *et al.* found the metastable minimum below $c/a<1$ to disappear using LDA.[13] They obtained the minimum only when GGA was used. However, Ayuela *et al.* obtained a global minimum around $c/a=1.25$, although the FPLAPW method has been used in Refs. 12 and 13. We have used the same parameters and GGA potential[25] for the FPLAPW calculations as in Ref. 13. Since, the energy differences between the global and local minima are small (Fig. 2), the disagreement between present results and that of Ayuela *et al.*[12,13] could arise due to the choice of parameters of calculation that are not generally mentioned explicitly and modifications of the WIEN97 code performed by them.[29] In our case, we have used the standard commercially available WIEN97 code[26] without any modifications.

Due to the above mentioned differences in literature about equilibrium c/a, we have performed E_{tot} minimization using a different method. In this iterative method,[30,31] in the first step a and c (i.e., the unit cell volume) are varied keeping c/a fixed at the experimental value of 0.94 [Fig. 3(a)]. The E_{tot} data are fitted with a fourth order polynomial, and from the minimum E_{tot}, an intermediate $a=a_{int}$ is obtained to be 11.23 a.u. Next, c/a is varied keeping $a=a_{int}$ fixed, and we obtain equilibrium (c/a) to be 0.95 [Fig. 3(b)]. At the third step, we again vary a and c with c/a fixed at 0.95 [Fig. 3(c)] and obtain the final equilibrium a and c to be 11.182 a.u. (5.915 Å) and 10.645 a.u. (5.631 Å), respectively with $c/a=0.95$. The small reduction in total energy at the different steps is clear from Figs. 3(a)–3(c).

The equilibrium c/a obtained from the iterative method (0.95) is somewhat smaller than that obtained from the constant volume method (0.97). However, the E_{tot} minimum in the iterative method is about 3.9 meV/atom higher than the constant volume method. Besides, the shapes of the different constant volume E_{tot} curves obtained by us show some differences. The dependence of E_{tot} curves on unit cell volume has also been reported earlier.[13] Because of the above mentioned complexities in this system, we employ a most general approach to obtain the E_{tot} minimum combining the results of both the constant volume and the iterative method. Besides, calculations have been done along a line joining the experimental (a,c) points of the austenitic and martensitic phases. Using all these E_{tot} data, we have constructed a two dimensional contour plot for E_{tot}, as functions of a and c [Fig. 4(a)]. More than 250 different calculations have been performed to obtain the contour plot. The general behavior of this system can be ascertained from Fig. 4(a). We find that along the c/a=constant direction (line B with $c/a=0.952$), E_{tot} increases rapidly, as depicted by closely spaced contours in that direction. Along the constant volume direction (for example, line C corresponding to the theoretically obtained equilibrium volume 1330.78 a.u.), E_{tot} variation is gradual and the contours are elongated along that direction (Fig. 4).

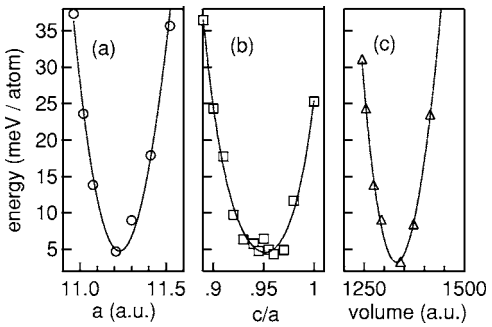

FIG. 3. E_{tot} of Ni_2MnGa in the martensitic phase using the iterative method (see text).

The minimum energy contour is shown by an arrow in Fig. 4(b), where the contour plot is shown in an expanded scale with finer contour spacing. The corresponding lattice constants and the equilibrium cell volume are determined at the middle of the contour and the extent of the contour along x and y give the error bars for a and c, respectively. Thus, we find $a=11.11\pm0.03$ a.u. (5.88 Å) and $c=10.78\pm0.025$ a.u. (5.70 Å), with $c/a=0.97$. This point is denoted by M in Fig. 4(b), representing the martensitic phase. a (5.88 Å) is within 0.7% of the experimental value of 5.92 Å and is thus in excellent agreement.[1,6,7] c (5.70 Å) is overestimated by 2.5% in theory w.r.t. experiment (5.56 Å).[1,6] Considering the experimental uncertainties of sample composition, homogenity and that the experiments are done at finite temperatures, this agreement can be considered to be very good. The equilibrium volume is obtained to be 1330.78 a.u. and E_{tot} as a function of c/a at this volume is shown in Fig. 2. We also obtain a local minimum around $a=11.22$ a.u. and $c=10.56$ a.u. from the contour plot [dashed arrow in Fig. 4(b)], where c/a is 0.94 as in experiment.[1,6,7] However, this local minimum is higher in energy from the global minimum by 5.5 meV/atom.

For the cubic austenitic phase, we have calculated E_{tot} by varying a. We obtain the equilibrium lattice constant to be 10.998 a.u. (5.820 Å) and is indicated by A in Fig. 4(b). The

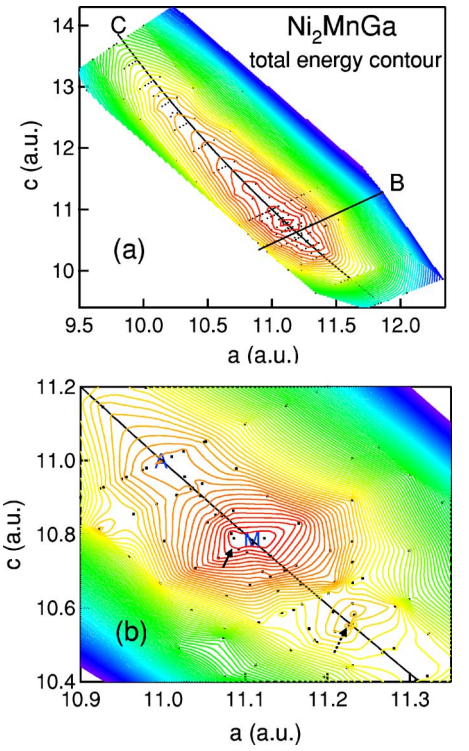

FIG. 4. (Color online) (a) E_{tot} of Ni_2MnGa in the martensitic phase as functions of a and c. In the gray scale (rainbow for color), the lightest (red) contour corresponds to minimum energy (0 mRy) and darkest (violet) corresponds to maximum energy (52 mRy or 176.8 meV/atom). The contour spacing is 1 mRy or 3.4 meV/atom. Black dots indicate the (a,c) points where calculations have been performed. Significance of lines B and C are discussed in text. (b) The contour plot around minimum E_{tot} in an expanded scale with finer contour spacing (0.1 mRy or 0.34 meV/atom). A solid arrow indicates the global minimum energy contour at $c/a=0.97$, while a dashed arrow indicates a local minimum energy contour at $c/a=0.94$. The equilibrium austenitic and martensitic phases are denoted by A and M, respectively.

lattice constant for the austenitic phase is in good agreement with our x-ray diffraction measurements (11.004 a.u.) and previous studies.[1,6,12,32] Comparing the minimum E_{tot} of the austenitic and the martensitic phases, we find that the latter is stabilized by 3.6 meV/atom. This shows why Ni_2MnGa undergoes a structural transition from cubic austenitic to tetragonal martensitic structure with decreasing temperature. The calculated volume of the austenitic phase is 1330.35 a.u., while that of the martensitic phase is 1330.78 a.u. Thus, the martensitic transition involves almost no change in volume, and this is evident from the contour plot in Fig. 4(b) where both the phases appear on the same constant volume curve (line C). This shows why Ni_2MnGa is a shape memory alloy, since volume conserving martensitic transition is a necessary and sufficient condition for shape memory effect in systems with cubic austentic phase.[33]

Ferromagnetism in Ni_2MnGa arises due to the RKKY type indirect exchange interaction between Mn atoms mediated by the Ni atoms.[19] From the FPLAPW calculation, we find the total magnetic moment in the austenitic phase to be 4.13 μ_B/f.u. and the individual moments per site for Ni, Mn,

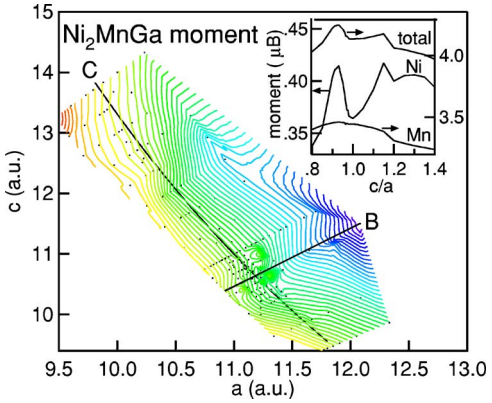

FIG. 5. (Color online) Total magnetic moment of Ni_2MnGa as functions of a and c. In the gray scale (rainbow for color), the lighest (red) contour corresponds to minimum: 3.8 μ_B and the darkest (violet) contour to maximum: 4.7 μ_B. The contour spacing is 0.02 μ_B and black dots indicate the (a,c) points where calculations have been performed. Inset shows the total, Mn and Ni magnetic moments as a function of c/a along line C.

and Ga are 0.36, 3.44, and −0.04 μ_B, respectively. These values are in agreement with previous theoretical studies.[9,10,12] For the equilibrium martensitic phase, the total moment is 4.16 μ_B, and the local moments per site are 0.37, 3.45, and −0.04 μ_B, respectively. The relatively small change in magnetic moment across the structural transition could be related to the spin-projected DOS, which is discussed later. The polarized neutron scattering results of Brown *et al.* normalized to 0 K gives moments of 0.24 and 2.74 μ_B for Ni and Mn, respectively in the austenitic phase, while moments in the martensitic phase are 0.36 and 2.83 μ_B, respectively.[20] The disagreement between experimentally determined moments and the zero temperature ideal moments calculated by us could be related to the existence of domain and twin structure, antisite defects, modulation, nonstoichiometry effects and orbital moments, which are not considered by theory. In Fig. 5, we show the total magnetic moment map of Ni_2MnGa as functions of c and a; while in the inset shows the total, Ni and Mn magnetic moment variation as a function of c/a for equilibrium volume (line C). Along line C, the total moment exhibits a maxima at $c/a=0.93$ and 1.15. Along line B, the total moment increases substantially up to about 4.7 μ_B for higher a and c ($\approx$12 a.u.). From the inset of Fig. 5, we find that the peaks in total moment are related to the changes in Ni moment, since Mn moment exhibits a smooth variation . The maximum in total and Ni moment around $c/a=0.93$ is more pronounced (4.25 μ_B) than that at 1.15 (4.17 μ_B), unlike in previous studies.[9,13] The variation in Ni magnetic moment can be related to changes in Ni spin-projected DOS close to E_F, as discussed later.

In Fig. 6, we show the total DOS and Ni 3d and Mn 3d partial density of states (PDOS) of Ni_2MnGa in the equilibrium martensitic and austenitic phases. The DOS is dominated by Ni and Mn 3d states in the bonding region below E_F. The shape and the total width ($\approx$6 eV) of the valence band is same for both the phases. The majority spin Ni 3d states extend from −4 eV to above E_F, and from PDOS calculations the t_{2g} and e_g states (not shown separately in Fig. 6)

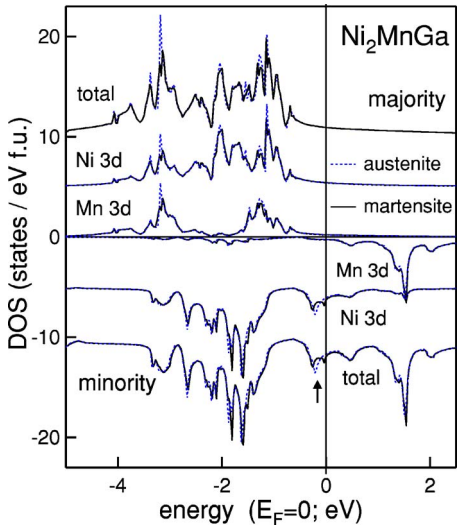

FIG. 6. (Color online) Majority and minority-spin total DOS and Ni 3*d* and Mn 3*d* PDOS of Ni_2MnGa in equilibrium austenitic and martensitic phases. The near E_F region (arrow) of the Ni 3*d* related minority-spin DOS exhibit interesting differences and is shown in an expanded scale in Fig. 7. The DOS curves are shifted along the vertical axis.

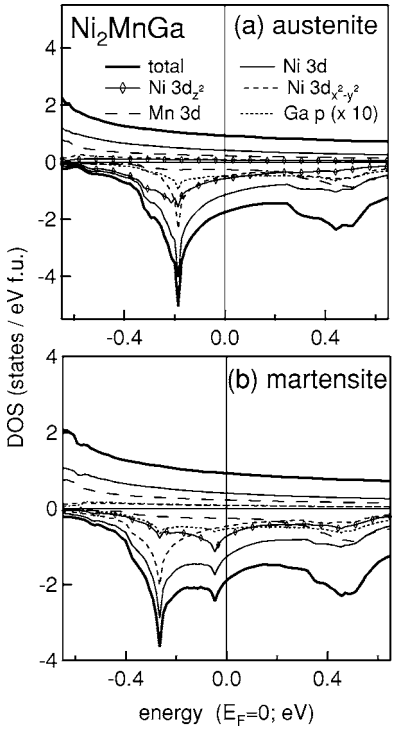

FIG. 7. Majority and minority-spin total DOS and PDOS of Ni_2MnGa in the near E_F region in equilibrium (a) austenitic and (b) martensitic phases. The Ga *p* PDOS is multiplied by a factor of 10.

are almost uniformly distributed. The minority-spin Ni 3*d* t_{2g} states are centered around −1.5 eV with a width of 0.6 eV. Ni 3*d* PDOS has a sizable contribution near E_F, which is primarily of e_g character. The minority-spin Mn 3*d* states dominate the antibonding region above E_F with the peak around 1.5 eV and has small contribution below E_F. Both Mn 3*d* t_{2g} and e_g states contribute equally to this peak. In contrast, the majority spin Mn 3*d* states are almost fully occupied and the t_{2g} and e_g states are clearly separated appearing at −3 and −1.3 eV, respectively.

An interesting difference between the two phases is observed near E_F (arrow, Fig. 6), which is shown in an expanded scale in Fig. 7. In the austenitic phase, the minority-spin DOS has a sharp peak around −0.19 eV. This peak is related to the Ni 3*d* e_g states, and in absence of tetragonal distortion both the $3d_{x^2-y^2}$ and $3d_{z^2}$ states appear at similar energies to contribute to this peak intensity. The Ga *p* PDOS, although much less in intensity, also has a peak at −0.19 eV, indicating a weak Ni *d*-Ga *p* hybridization. The peak centered at 0.45 eV above E_F arises from Ni 3*d*-Mn 3*d* hybridized states. The majority spin states have a monotonically decreasing DOS towards E_F with no structure. Due to the tetragonal distortion in the martensitic phase, the Ni minority-spin 3*d* e_g PDOS splits into two peaks [Fig. 7(b)]. The −0.27 eV peak is dominated by Ni $3d_{x^2-y^2}$ with a small contribution from the $3d_{z^2}$ states. On the other hand, the −0.05 eV peak is almost entirely related to the $3d_{z^2}$ states. The Ga *p* PDOS also exhibits a similar splitting as the Ni e_g states. In contrast, Mn 3*d* PDOS does not exhibit any feature at −0.27 or −0.05 eV. The martensitic phase has lower energy probably because the higher intensity Ni $3d_{x^2-y^2}$ dominated peak appears at lower energy (−0.27 eV) compared to the austenitic phase (−0.19 eV).

Fujii *et al.* calculated the DOS of both martensitic and austenitic phases using the Korringa-Kohn-Rostocker method and suggested that the band Jahn-Teller effect stabilizes the martensitic phase.[10] A signature of the band Jahn-Teller effect is splitting of a peak exactly at E_F into two peaks below and above E_F resulting in a lowering of total energy. However, our results clearly show that, although splitting occurs, both the split peaks are below E_F. So, the stabilization of the martensitic phase is related to the lowering of the total energy and cannot be described purely in terms of the band Jahn-Teller effect. Magnetic moment is determined by the difference between the integrated occupied majority and minority-spin DOS. Since both Ni $3d_{z^2}$ and $3d_{x^2-y^2}$ states are below E_F in the martensitic phase, the occupancy of Ni spin-projected states does not change substantially compared to the austenitic phase. This explains the small change in Ni magnetic moment across the martensitic transition. The small change in Mn moment can be explained in a similar way (Fig. 6).

In Fig. 8, we plot the total majority and minority-spin DOS at E_F as a function of c/a for equilibrium volume. We find a large variation in the minority-spin DOS with two peaks at 0.96 and 1.1. These peaks can be related to the changes in the DOS with c/a: when c/a decreases below 1, the Ni $3d_{z^2}$ related peak shifts toward E_F and at 0.96 it passes through E_F. On the other hand, when c/a increases, the Ni $3d_{x^2-y^2}$ peak shifts towards E_F and passes through E_F at 1.1. In contrast, the majority spin states exhibit almost no change over the whole range. The maxima in Ni magnetic moment at $c/a=0.93$ and 1.15 (inset, Fig. 5) are related to the variation in the minority-spin DOS with c/a. We show that in Ni_2MnGa, the minority-spin DOS at E_F is sensitive to change in lattice constants, while the majority spin DOS is not.

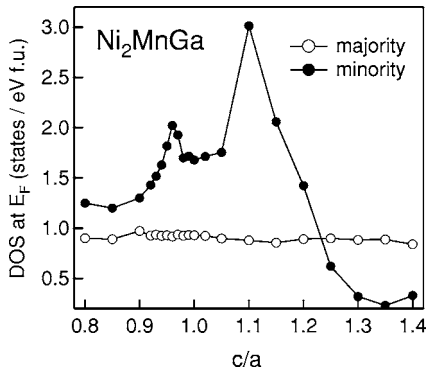

FIG. 8. Total majority and minority-spin DOS at E_F of Ni_2MnGa as a function of c/a for the equilibrium volume (1330.78 a.u.).

IV. CONCLUSION

We have determined the optimized lattice constants and the electronic structure of Ni_2MnGa using the full potential linearized augmented plane wave (FPLAPW) method. We show that the equilibrium tetragonal martensitic phase with $c/a=0.97$ has 3.6 meV/atom lower energy than the austenitic phase, which explains why the martensitic transition occurs in Ni_2MnGa by lowering the temperature. This result is important because until now no global minimum for $c/a<1$ has been obtained for the martensitic phase of Ni_2MnGa. We find the martensitic phase lattice constants to be $a=11.11\pm0.03$ a.u. (5.88 Å) and $c=10.78\pm0.03$ a.u. (5.70 Å), which are in good agreement with experiment. The martensitic transition is volume conserving, as expected for a shape memory alloy. The present results show that it is indeed possible to obtain the stable martensitic phase in Ni_2MnGa without considering extraneous effects like modulation, nonstoichiometry, shuffle or distortion. By comparing the DOS of the two phases, we find a splitting of the minority-spin states below E_F. These states are predominantly Ni 3*d*-like, weakly hyrbidized with Ga*p*-like states. The total, Ni and Mn magnetic moments in the martensitic phase are reported as function of the lattice constants and related to the spin-projected DOS. The minority-spin DOS at E_F varies with c/a, while the majority spin DOS is unaffected. This could have important implication in spin polarized transport where the tunability of the minority-spin DOS can be used. This also shows that surface relaxation and change in structure at the interfaces might change the efficiency of spin polarized transport. A decrease in the minority-spin DOS near E_F for Ni excess $Ni_{2.25}Mn_{0.75}Ga$ has been recently reported.[34]

ACKNOWLEDGMENTS

Dr. P. Kratzer and Professor K. Kunc are thanked for useful discussions. Dr. K. C. Rustagi, Dr. P. Chaddah, Professor K. Horn, Professor A. Gupta, and Mr. T. P. S. Nathan are thanked for constant encouragement. The Department of Science and Technology, India and Max Planck Gesellschaft, Germany are thanked for financial support.

*Electronic address: barman@csr.ernet.in; srbarman@mailcity.com

[1] P. J. Webster, K. R. A. Ziebeck, S. L. Town, and M. S. Peak, Philos. Mag. B **49**, 295 (1984).
[2] A. Sozinov, A. A. Likhachev, N. Lanska, and K. Ullakko, Appl. Phys. Lett. **80**, 1746 (2002).
[3] J. Marcos, L. Mañosa, A. Planes, F. Casanova, X. Batlle, and A. Labarta, Phys. Rev. B **68**, 094401 (2003).
[4] X. Zhou, W. Li, H. P. Kunkel, and G. Williams, J. Phys.: Condens. Matter **16**, L39 (2004).
[5] C. Biswas, R. Rawat, and S. R. Barman, Appl. Phys. Lett. **86**, 202508 (2005); cond-mat/0412646.
[6] B. Wedel, M. Suzuki, Y. Murakami, C. Wedel, T. Suzuki, D. Shindo, and K. Itagaki, J. Alloys Compd. **290**, 137 (1999).
[7] V. V. Martynov and V. V. Kokorin, J. Phys. III **2**, 739 (1992).
[8] P. J. Brown, J. Crangle, T. Kanomata, M. Matsumoto, K.-U. Neumann, B. Ouladdiaf, and K. R. A. Ziebeck, J. Phys.: Condens. Matter **14**, 10159 (2002).
[9] V. V. Godlevsky and K. M. Rabe, Phys. Rev. B **63**, 134407 (2001).
[10] S. Fujii, S. Ishida, and S. Asano, J. Phys. Soc. Jpn. **58**, 3657 (1989).
[11] O. I. Velikokhatnyi and I. I. Nuamov, Phys. Solid State **41**, 617 (1999).
[12] A. Ayuela, J. Enkovaara, K. Ullakko, and R. M. Nieminen, J. Phys.: Condens. Matter **11**, 2017 (1999).
[13] A. Ayuela, J. Enkovaara, and R. M. Nieminen, J. Phys.: Condens. Matter **14**, 5325 (2002).
[14] J. M. MacLaren, J. Appl. Phys. **91**, 7801 (2002).
[15] C. Bungaro, K. M. Rabe, and A. Dal Corso, Phys. Rev. B **68**, 134104 (2003).
[16] A. T. Zayak, P. Entel, J. Enkovaara, and R. M. Nieminen, J. Phys.: Condens. Matter **15**, 159 (2003); A. T. Zayak and P. Entel, Mater. Sci. Eng., A **348**, 419 (2004).
[17] J. Pons, V. A. Chernenko, R. Santamarta, and E. Cesari, Acta Mater. **48**, 3027 (2000).
[18] N. Lanska, O. Söderberg, A. Sozinov, Y. Ge, K. Ullakko, and V. K. Lindroos, J. Appl. Phys. **95**, 8074 (2004).
[19] J. Kübler, A. R. Williams, and C. B. Sommers, Phys. Rev. B **28**, 1745 (1983).
[20] P. J. Brown, A. Y. Bargawi, J. Crangle, K.-U. Neumann, and K. R. A. Ziebeck, J. Phys.: Condens. Matter **11**, 4715 (1999).
[21] A. Deb, M. Itou, Y. Sakurai, N. Hiraoka, and N. Sakai, Phys. Rev. B **63**, 064409 (2001); A. Deb, N. Hiraoka, M. Itou, Y. Sakurai, M. Onodera, and N. Sakai, *ibid.* **63**, 205115 (2001).
[22] E. Zukowski, A. Andrejczuk, L. Dobrzynski, M. J. Cooper, M. A. G. Dixon, S. Gardelis, P. K. Lawson, T. Buslaps, S. Kaprzyk, K.-U. Neumann, and K. R. A. Ziebeck, J. Phys.: Condens. Matter **9**, 10993 (1997).
[23] A. Kimura, S. Suga, T. Shishidou, S. Imada, T. Muro, S. Y. Park, T. Miyahara, T. Kaneko, and T. Kanomata, Phys. Rev. B **56**, 6021 (1997); A. Yamasaki, S. Imada, R. Arai, H. Utsunomiya, S. Suga, T. Muro, Y. Saitoh, T. Kanomata, and S. Ishida, *ibid.* **65**,

104410 (2002); K. Miyamoto, A. Kimura, K. Iori, K. Sakamoto, T. Xie, T. Moko, S. Qiao, M. Taniguchi, and K. Tsuchiya, J. Phys.: Condens. Matter **16**, S5797 (2004).

[24] G. Bihlmayer, R. Eibler, and A. Neckel, Philos. Mag. B **73**, 511 (1996).

[25] J. P. Perdew, K. Burke, and M. Ernzerhof, Phys. Rev. Lett. **77**, 3865 (1996).

[26] P. Blaha, K. Schwartz, and J. Luitz, WIEN97, A Full Potential Linearized Augmented Plane Wave Package for Calculating Crystal Properties (Karlheinz Schwarz, Tech. Universität, Wien, Austria), 1999. ISBN 3–9501031–0-4.

[27] S. Picozzi, A. Continenza, and A. J. Freeman, Phys. Rev. B **66**, 094421 (2002).

[28] A. Deb and Y. Sakurai, J. Phys.: Condens. Matter **12**, 2997 (2000).

[29] J. Enkovaara, dissertation 119, Helsinki University of Technology (2003) (http:lib.hut.fi/Diss/2003/isbn951226319X/isbn951226319X.pdf), p. 17.

[30] A. Chakrabarti, K. Hermann, R. Druzinic, M. Witko, F. Wagner, and M. Petersen, Phys. Rev. B **59**, 10583 (1999).

[31] A. Chakrabarti, Phys. Rev. B **62**, 1806 (2000).

[32] C. Biswas, G. S. Okram, A. M. Awasthi, N. P. Lalla, and S. R. Barman, in Proceedings of DAE Solid State Physics Symposium (2002), Vol. 45, p. 439.

[33] K. Bhattacharya, *Microstructure of Martensite. Why it Forms and How it Gives Rise to the Shape-Memory Effect* (Oxford University Press, Oxford, 2003).

[34] A. Chakrabarti, C. Biswas, S. Banik, R. S. Dhaka, A. K. Shukla, and S. R. Barman, Phys. Rev. B **72**, 073103 (2005).